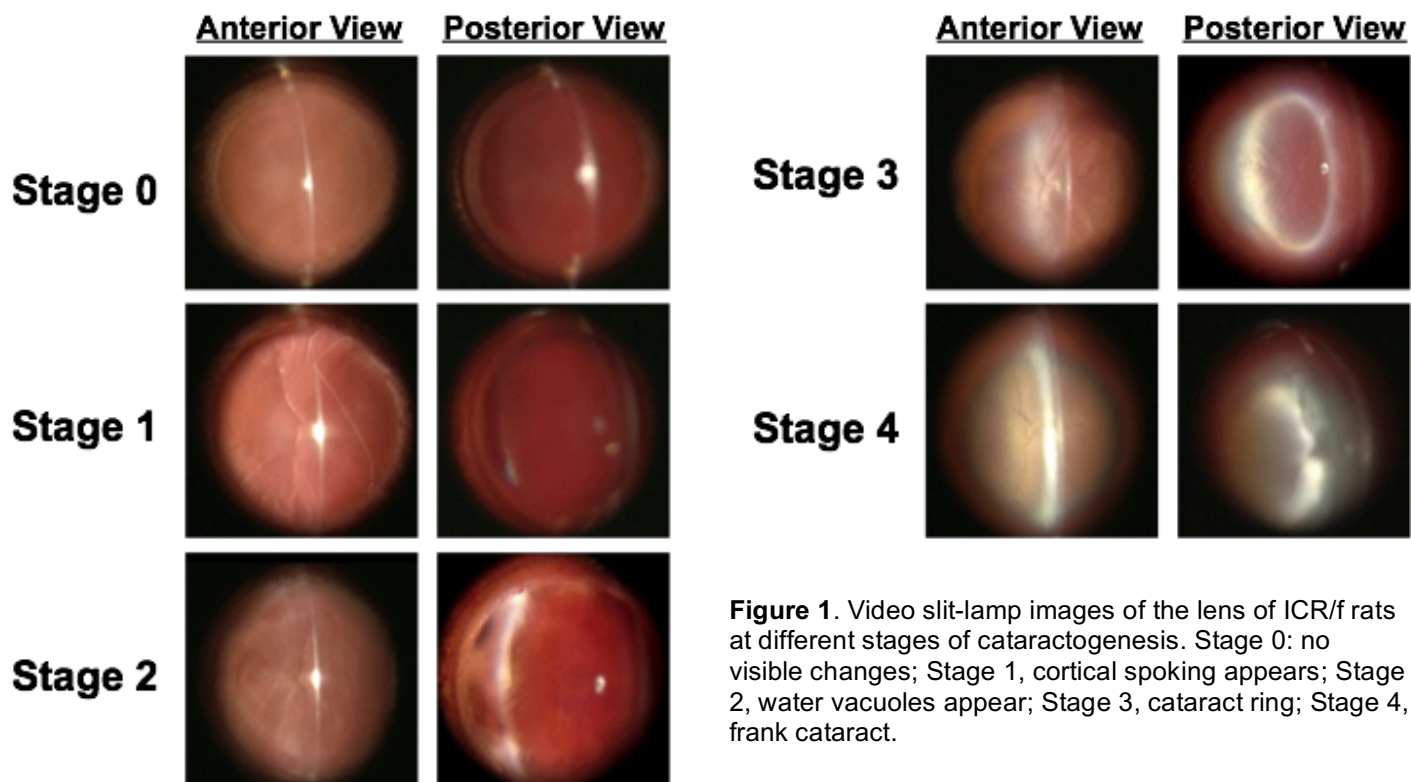Key reagents to be used in this proposal.

1. The ICR/f rat model of cataractogenesis

This animal strain (Ihara's cataractous rat) was obtained from investigators at Meijo University in Japan in 2005. They sent us four female rats and two male rats and we built a colony which been maintained ever since. All the animals born develop bilateral cataracts by 85 days of age. The original rat in the ICR series was first described in 1981 [1] and it's been well characterized [2]. Full genomic sequencing of this strain is yet to be reported so that the nature of the genetic defects causing the cataracts are unknown. However, a recessive mutation responsible for cataract development was localized to the Cati1 gene loci on chromosome 8 which also contains the APOCIII gene which is responsible for lipoprotein metabolism [3]. The ICR/f rat has neutropenia and eosinophilia and there is a significant surge of serum lipid peroxide levels on day 13 after birth (when blood vessels are still perfusing the lens) which returned to normal levels by day 17 [2]. These authors concluded that this rapid oxidative insult caused irreparable damage to the lens leading to the future development of cataracts [2] and that this model can be used to study age-related cataract. The Cati1 gene was found to determine the presence of cataracts within the IER rat, while another gene (Cati2) was discovered on chromosome 15. Cati2 was found to determine whether the animal had a rapid onset of cataract or a late onset [3].

Figure 1. Video slit-lamp images of the lens of ICR/f rats at different stages of cataractogenesis. Stage 0: no visible changes; Stage 1, cortical spoking appears; Stage 2, water vacuoles appear; Stage 3, cataract ring; Stage 4, frank cataract.

We have used the ICR/f rat in two published studies. We decided to do this on the basis of a study showing that grape seed extract containing procyanidins reduced the development of lens cataract in the latter stages of cataractogenesis [4]. Funded by R21 (EY020963 from NEI) and P50 (AT00477 from NCCAM, now NCCIH, and the Office of Dietary Supplements) grants we were unable to reproduce these results [5]. Using the model, we went on to show that the presence of soy isoflavones in the diet (typically what is in laboratory chow diets) accelerated the onset of the earlier stages (I and II) of cataractogenesis in this model [5] – see Fig. 1 above. Unlike the Japanese group, we collected slit lamp videos from the time that the animals were placed on the test diets. This captured the earlier stages that they missed. We also used the model to test whether disulfiram given as eye drops could prevent cataracts as per an earlier study [6]. Again, we were unable to confirm this result.

Where the ICR/f rat has proved to be very useful is in imaging mass spectrometry of the lens proteins during aging [7], a study funded by NEI R21 EY020963. We went on the develop new technologies form maintaining the localization of proteins within the lens [8]. We also worked with several other colleagues in the lens field to show that many other lens proteins form concentric rings within the lens. With regard to reproducibility, the figure below shows the consistency of our findings.
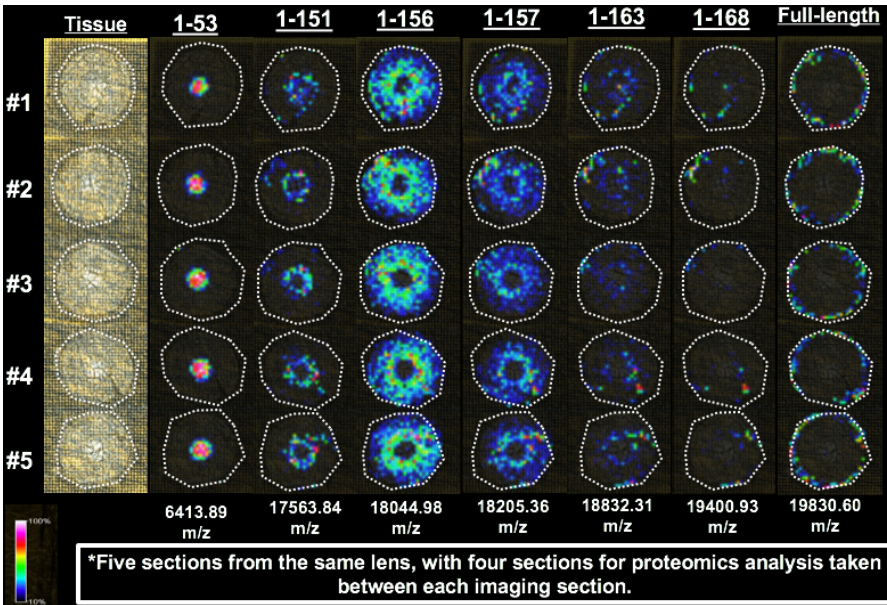

Figure 2. Reproducibility of the imaging-MS patterns of frozen sections of ICR/f rat lens. The 1-53 aa αA-crystallin is only found in the nuclear region; the 1-151 aa and 1-56 aa αA-crystallins form a band around the nuclear region which is found diffusely through the cortical region; the full-length αA-crystallin is confined to the newly formed epithelial cells on the surface of the lens.
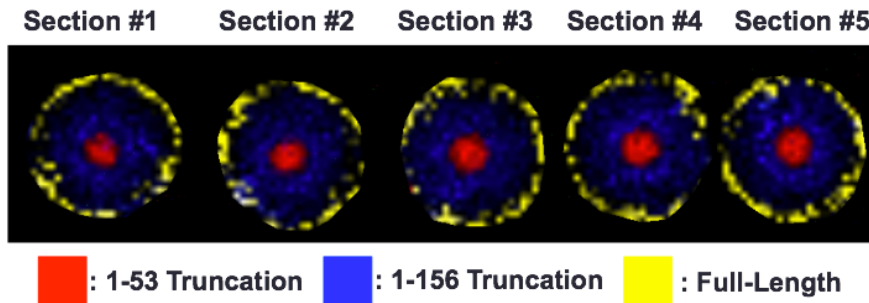
Figure 3. Summation of the images various forms of αA-crystallin from Figure 2 shows that the interpretation of the data is consistent.

2. Lipid imaging mass spectrometry

All reagents for tissue preparation andmatrix application by vacuum sublimation for lipid imaging mass spectrometry are purchased from commercial vendors. Reproducibility of this method has been assured through our prior studies, including one recently published in American Journal of Physiology-Renal in which lipid changes associated with early stages of acute kidney injury were localized using the lipid imaging method proposed in this application [9]. As per the proteins in Figs. 1 and 2), we have confirmed the reproducibility of our lipid imaging method by performing 10 separate imaging runs on 10 cryosections obtained from the eye of the same mouse and determined that the spectra obtained were identical in terns of both the number and the relative intensities of major lipid ions. Furthermore, we were able to confirm that the same lipid (16:0/20:4 PC) localized to the same outermost regions of the eye lens and the same retinal lamellae in each of these imaging experiments (as seen in **Figure 3**).
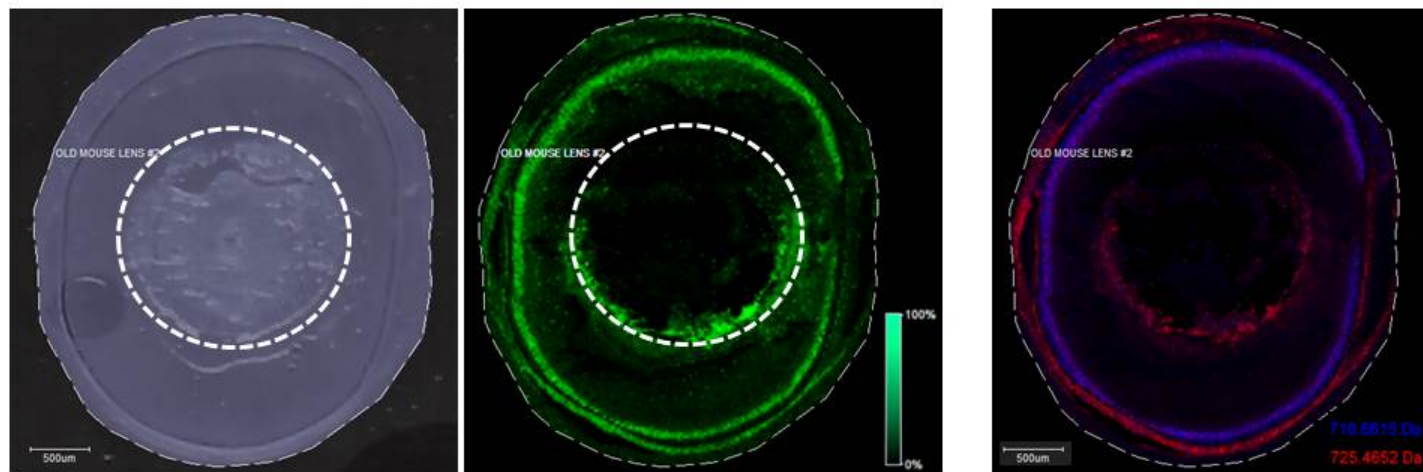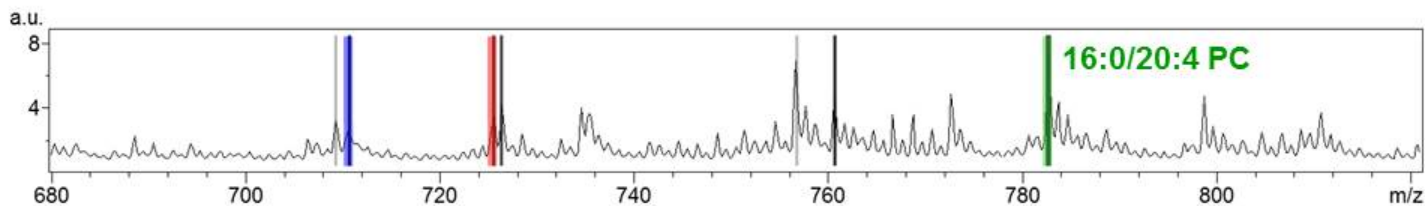
Figure 3. MALDI-IMS of three lipid ions in aged mouse eye. 16:0/20:4 PC localization is shown in green. Two other yet to be identified ipid s ith *m/z* values of 710.6615 (blue) and 725.4652 (red) are shown in the right panel. Note their distinct locations within different retinal lamellae.

3. MSMS[ALL] of lipids

We have used this comprehensive, infusion-based, MSMS method in several studies, three of which have been recently published [9-11]. The typical procedure that we've used is as follows (as per ref 11):

Approximately 100 µL of diluted lens lipid extract in methanol:chloroform (2:1, v/v) containing 5 mM ammonium acetate is infused isocratically at a flow rate of 7 µL/min using a 500 µL Hamilton Gas Tight Syringe. Syringe cleaning is essential, prior to and in between samples. The direct syringe is cleaned with multiple solvents. The solvent wash steps include two flushes with 100% methanol, two flushes with 100% acetonitrile, two flushes with 100% isopropyl alcohol, and two flushes with 100% direct infusion solvent. Calibration standards, APCI Positive Calibration Solution (Part # 4460131) and APCI Negative Calibration Solution (Part# 4460134), for direct infusion analyses are provided by SCIEX. Positive and negative ion MS and MS/MS spectra are carried out using a Triple TOF™ 5600 System (SCIEX, Concord, ON, Canada). Initially, a 250 msec high resolution TOF scan is acquired over *m/z* 200-1200. Then a series of 100 msec high sensitivity product ion scans are acquired using overlapping *m/z* 1.2 windows starting at *m/z* 200 and increasing in 1 *m/z* steps through 1200 *m/z*. The collision energy is 35 V, curtain gas 20, GS1 and GS2 to 15, spray voltage to 5500 V (positive ion mode)/4500 V (negative ion mode), and temperature to 400 °C. The total time to carry out the entire experiment is ~6 min.

The acquired TOF MS and MS/MS data are processed with LipidView™ 1.2 software (SCIEX, Concord, ON, Canada). LipidView™ assigns lipid identities based on a fragmentation database. To further investigate ions and confirm selected identities, neutral loss or precursor ion scans are carried out using PeakView™ 1.2 software (SCIEX, Concord, ON, Canada). The mass tolerance window for processing is 5 mDa and the peaks in MS/MS scans greater than signal-to-noise of 3 are considered. Identification of individual lipid species from LipidView™ assignments was based on mass accuracy (<5 ppm) and MS/MS spectra obtained from PeakView™. High resolution TOF-MS spectra provide the accurate mass of precursor ions. MarkerView™ 1.21 software (SCIEX, Concord, ON, Canada) is used to visualize trends across replicates and groups. Statistical analysis (univariate - Volcano plots and multivariate - Principal components analysis) is performed to establish and visualize the

similarities and differences within and between groups, based on LipidView™ assignments. We have found that n=6 samples measured in duplicate provides acceptable reproducibility [11].

Where necessary, we will use FT-ICR-MS analysis to obtain more accurate estimates of mass since there are many overlapping peaks due to natural abundance ^{13}C. We have found that some of these problems can be overcome using the SelexION interface of the SCIEX 6500 Qtrap. In this mode, classes of lipids can be separated by differential mobility mass spectrometry. In the example shown below, a CHCl$_3$:MeOH plasma extract was infused without further purification. Precursor ions giving rise to the phosphocholine product ion (*m/z* 184.07) were subjected to different compensation voltages (Fig. 4A). Then MS precursor ion spectra were obtained at selected compensation voltages (Figs. 4B-D).
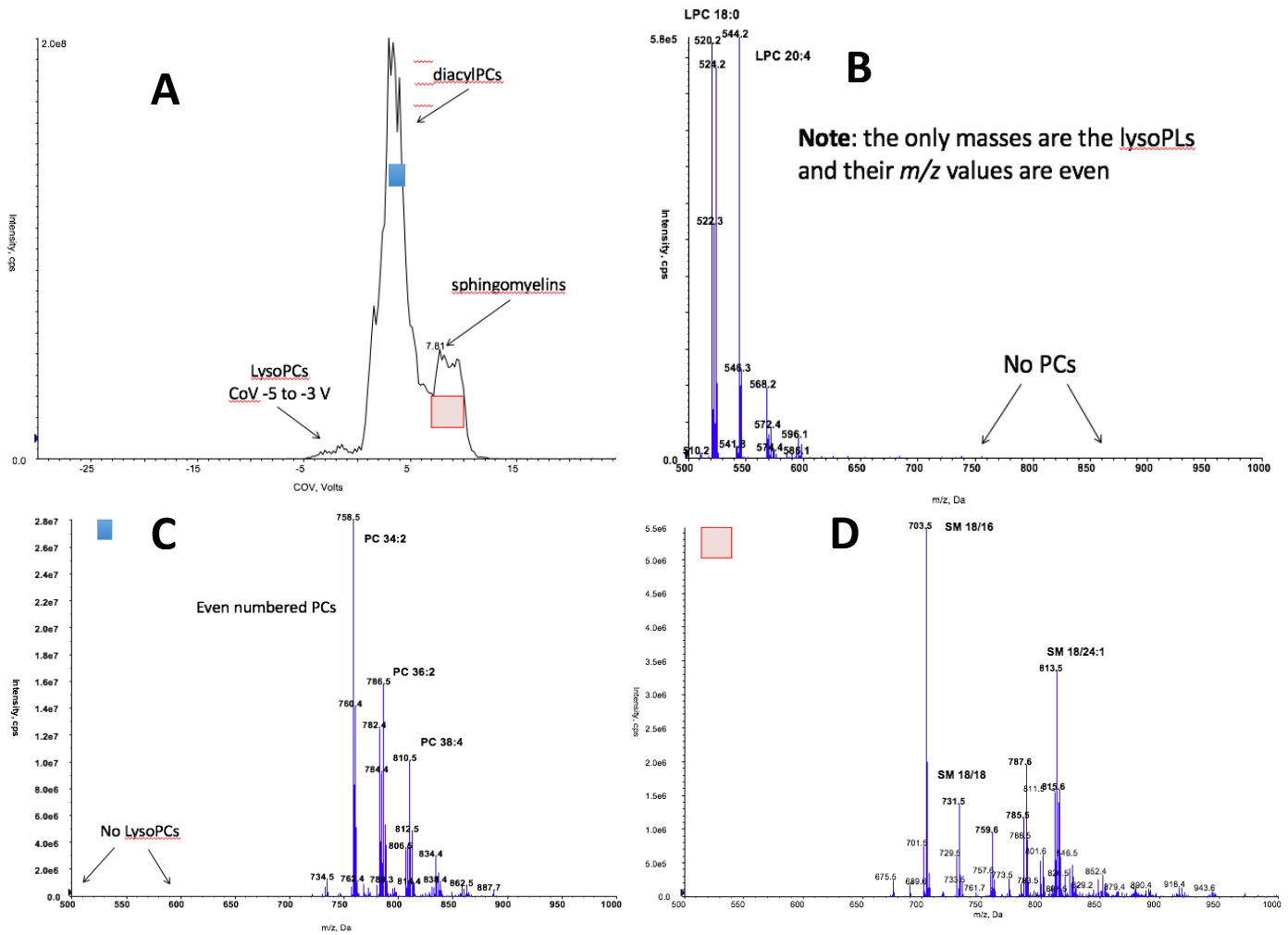
Figure 4. Differential ion mobility mass spectrometry of plasma lipids (positive mode). The precursor ions that give rise to the m/z 184.07 product ion (phosphocholine) were scanned using a compensating voltage (CoV) from -30 to 20 V (Figure A). Setting the CoV to -3.6 to -0.6 V (Figure B) isolated the lysophospholipids with none of the diacyl phospholipids. Adjusting the CoV to 3.0 to 3.6 V (Figure C) separated the phosphatidylcholines (even numbered) from the sphingomyelins (odd numbered). Similarly, adjustment of the CoV to 7.8 to 10 V separated the sphingomyelins from the phosphatidylcholines.

References

1. Ihara, N. A new strain of rat with an inherited cataract. *Experimentia*, 1983;39: 909-911.
2. Nishida S, Mizuno K, Matubara A, Kurno M. Age-related cataract in the hereditary cataract rat (ICR/1): development and classification. *Opthalmic Research* 1992;24: 253-259.
3. Yokoyama M, Amano S, Tsuji A, Sasahara M, Serikawa T, Ihara N, Matsuda M, Hazama F, Handa J. Genetic analysis of cataract in Ihara epileptic rat. *Mammalian Genome*, 2001;12: 207-211.

4. Yamakoshi J, Saito M, Kataoka S, Tokutake S. Procyanidin-rich extract from grape seeds prevents cataract formation in hereditary cataractous (ICR/f) rats. *J Agric Food Chem*. 2002;50:4983-8.
5. Floyd KA, Stella DR, Wang CC, Laurentz S, McCabe GP, Srivastava OP, Barnes S. Genistein and genistein-containing dietary supplements accelerate the early stages of cataractogenesis in the male ICR/f rat. *Exp Eye Res*. 2011 Feb;92(2):120-7.
6. Nagai N, Ito Y, Takeuchi N. Pharmacokinetic and pharmacodynamic evaluation of the anti-cataract effect of eye drops containing disulfiram and low-substituted methylcellulose using ICR/f rats as a hereditary cataract model. *Biol Pharm Bull*. 2012;35(2):239-45.
7. Stella DR, Floyd KA, Grey AC, Renfrow MB, Schey KL, Barnes S. Tissue localization and solubilities of αA-crystallin and its numerous C-terminal truncation products in pre- and postcataractous ICR/f rat lenses. *Invest Ophthalmol Vis Sci*. 2010 Oct;51(10):5153-61.
8. Anderson DM, Floyd KA, Barnes S, Clark JM, Clark JI, Mchaourab H, Schey KL. A method to prevent protein delocalization in imaging mass spectrometry of non-adherent tissues: application to small vertebrate lens imaging. *Anal Bioanal Chem*. 2015 Mar;407(8):2311-20.
9. Rao S, Walters KB, Wilson L, Chen B, Bolisetty S, Graves D, Barnes S, Agarwal A, Kabarowski JH. Early lipid changes in acute kidney injury using SWATH lipidomics coupled with MALDI tissue imaging. *Am J Physiol Renal Physio*l. 2016 Feb 24:ajprenal.00100.2016. doi: 10.1152/ajprenal.00100.2016. [Epub ahead of print]
10. Xie X, Wang X, Mick GJ, Kabarowski JH, Shay Wilson L, Barnes S, Walcott GP, Luo X, McCormick K. Effect of n-3 and n-6 Polyunsaturated Fatty Acids on Microsomal P450 Steroidogenic Enzyme Activities and In Vitro Cortisol Production in Adrenal Tissue from Male Yorkshire Boars. *Endocrinology*. 2016 Feb 18:en20151831. [Epub ahead of print]
11. Prasain JK, Wilson L, Hoang HD, Moore R, Miller MA. Comparative Lipidomics of Caenorhabditis elegans Metabolic Disease Models by SWATH Non-Targeted Tandem Mass Spectrometry. *Metabolites*. 2015 Nov 11;5(4):677-96.